Journal of Clinical and Translational Hepatology **2022** vol. 10(2) | 207–218
DOI: 10.14218/JCTH.2021.00101

Original Article

KRT17 Promotes the Activation of HSCs via EMT in Liver Fibrosis

Jing Chen[1,2#], Si-Jia Ge[1,2#], Hai-Juan Feng[1,2], Shu-Zhen Wu[1,2], Ran Ji[1,2], Wei-Rong Huang[1,2], Wei Huang[1*] and Cui-Hua Lu[1*]

[1]Department of Gastroenterology, Affiliated Hospital of Nantong University, Nantong, China; [2]Research Center of Clinical Medicine, Nantong University, Affiliated Hospital of Nantong University, Nantong, China

Received: 21 March 2021 | **Revised:** 19 May 2021 | **Accepted:** 6 June 2021 | **Published:** 8 July 2021

Abstract

Background and Aims: Although activation of hepatic stellate cells (HSCs) plays a central role in the development of liver fibrosis, the mechanism underlying the activation of HSCs remains unclear. Keratin 17 (KRT17), a member of the intermediate filament family, can regulate tumor cell proliferation and migration. The current study aimed to elucidate the role of KRT17 in the activation of HSCs and the mechanisms underlying liver fibrosis. ***Methods:*** The expression of KRT17 was determined using immunohistochemistry in tissue microarray. Western blotting and qRT-PCR assays were used to determine the KRT17 expression in fibrotic liver tissues obtained from human subjects and mice. LX-2 cells were treated with TGF-β1 recombinant protein and adipocyte differentiation mixture (MDI) mix to induce and reverse LX-2 cell activation, respectively, in order to explore the correlation between KRT17 and HSC activation. Additionally, cell proliferation and migration abilities of LX-2 cells transfected with KRT17-overexpressing plasmid or small interfering RNA were determined using CCK-8, flow cytometry, Transwell, and wound healing assays. Finally, rescue assay was used to explore the role of KRT17 in HSC activation and epithelial-mesenchymal transition (EMT). ***Results:*** The expression of KRT17 was higher in the human and mouse fibrotic liver tissues than in healthy liver tissues, and it was positively correlated with HSC activation. Upregulated KRT17 enhanced proliferation, migration, HSC activation and EMT in LX-2 cells, while knockdown of KRT17 reversed these effects. TGF-β1 recombinant protein accelerated KRT17-mediated EMT, HSC activation and proliferation, while TGF-β1 inhibitor counteracted the effect of KRT17 *in vitro*. ***Conclusions:*** KRT17 promoted HSC activation, proliferation and EMT in hepatic fibrosis probably via TGF-β1 signaling, and KRT17 might serve as a therapeutic target for the treatment of liver fibrosis.

Citation of this article: Chen J, Ge SJ, Feng HJ, Wu SZ, Ji R, Huang WR, *et al*. KRT17 Promotes the Activation of HSCs via EMT in Liver Fibrosis. J Clin Transl Hepatol 2022;10(2):207–218. doi: 10.14218/JCTH.2021.00101.

Introduction

Hepatic fibrosis, as a consequence of persistent liver damage induced by multiple etiologies, including viral hepatitis, cholestatic liver diseases, alcoholism, metabolic disorder and autoimmune conditions,[1,2] is a protective wound-healing response featuring extracellular matrix (ECM) deposition generated by activated hepatic stellate cells (HSCs).[3,4] The incidence of hepatic fibrosis is increasing rapidly across the world.[5] HSCs have generally been corroborated to be the main source of ECM-producing myofibroblasts, independent of its etiology.[6] Increasing evidence shows that during the process of hepatic fibrosis, HSCs, which contain retinal lipid droplets, obtain a myofibroblast-like phenotype and transdifferentiate into myofibroblasts, and possess contractile, proliferative and fibrogenic properties.[7,8]

This process is known as HSC activation, and it leads to the ECM hyperplasia characterized by the expression of α-smooth muscle actin (α-SMA), type I collagen alpha 1(Col1α1), and type III collagen alpha 1 (Col3α1).[9,10] Notably, liver fibrosis progresses gradually and is reversible.[11] However, repeated injuries can lead to fundamental remodeling of hepatic architecture and the destruction of healthy liver function by orchestrated signaling networks.[12] They can ultimately result in more serious liver pathologies, including cirrhosis, liver dysfunction, and end-stage hepatocellular carcinoma (HCC), which is difficult to reverse and causes severe morbidity worldwide.[13,14] So far, we have witnessed enormous progress in understanding the pathogenic mechanisms underlying hepatic fibrosis. However, we are yet to uncover the complicated mechanisms that can provide new insights into this disease to treat it effectively.

Epithelial-mesenchymal transition (EMT) is a multistep and dynamic process, during which phenotypic characteristics of epithelial cells, including intercellular adhesion and cell polarity, are lost.[15] It is also noteworthy to mention that they transform into mesenchymal cells, such as fibroblasts,

Keywords: KRT17; Hepatic stellate cell activation; Liver fibrosis; Epithelial–mesenchymal transition; TGF-β signaling.

Abbreviations: α-SMA, α-smooth muscle actin; CCK-8, Cell Counting Kit-8; CCl_4, carbon tetrachloride; Col1α1, type I collagen alpha 1; Col3α1, type III collagen alpha 1; DAB, 3, 3′-diaminobenzidine tetrahydrochloride; ECM, extracellular matrix; EMT, epithelial-mesenchymal transition; H&E, hematoxylin and eosin; H_2O_2, hydrogen peroxide; HCC, hepatocellular carcinoma; HSCs, hepatic stellate cells; KRT17, keratin 17; MDI, adipocyte differentiation mixture; RT-qPCR, real-time quantitative polymerase chain reaction; PI, propidium iodide; SE, standard error; siRNA, small interfering RNA; TMA, tissue microarray.

[#]Contributed equally to this work.

[*]**Correspondence to:** Wei Huang and Cui-Hua Lu, Department of Gastroenterology, Affiliated Hospital of Nantong University, Nantong, China. ORCID: https://orcid.org/0000-0001-8471-530X (WH), https://orcid.org/0000-0002-1377-5820 (CHL). Tel: +86-13962991839 (WH), +86-13962801685 (CHL), Fax: +86-513-8116-1826, E-mail: huangweint@ntu.edu.cn (WH), lch670608@sina.com (CHL)

and acquire migratory and invasive properties.[16] Recent research suggested that EMT plays an important role in wound healing and liver fibrosis.[17] HSCs in the liver can facilitate their transformation into myofibroblasts and accelerate the proliferation of HSCs via EMT, thus contributing to hepatic fibrogenesis through the deposition of ECM in the liver.[18] Among numerous mediators concerned with the initiation of EMT and fibrogenesis, TGF-β1 is a critical multifunctional cytokine that is produced by injured hepatocytes and plays pivotal roles in the activation of HSCs and their transformation to myofibroblasts.[19,20] The fibrogenic activation of HSCs by TGF-β1 stimulates self-expression and that of the other cytokines, consequently exacerbating liver fibrosis.[21] TGF-β1 also favors the EMT of HSCs actions to aggravate liver fibrosis, which is characterized by the increased production of collagen and ECM by HSCs.[22]

Keratin 17 (KRT17) is a type I keratin protein with a molecular weight of 48 kDa.[23] It belongs to the intermediate filament family and contains four transmembrane domains that make up the cytoskeleton,[24] which is critical for cell protection and structural support.[25] It was found that KRT17 is generally distributed in epithelial basal cells and cutaneous appendages.[26] It can be induced in the environment following intense inflammation, thereby protecting epithelial cells from damage or physical stress and maintaining their integrity.[27] An increase in KRT17 expression was observed in several malignant epithelial tumor tissues and it may function as a diagnostic marker for diseases such as breast carcinoma, skin squamous cell carcinoma, and gastric cancer. KRT17 is strongly related to tumorigenesis and poor prognosis of these cancers.[28,29] Furthermore, the occurrence of EMT is shown to be closely associated with the overexpression of KRT17, implying a significant role of KRT17 in boosting actin reorganization, proliferation, migration, and the formation of the malignant phenotype in carcinoma cells.[30,31] Nonetheless, the answer as to whether KRT17 affects EMT and activates HSCs in liver fibrosis remains elusive. Similarly, the regulation of KRT17 expression in hepatic fibrosis is not well understood. Therefore, to improve the early diagnosis and treatment of hepatic fibrosis, uncovering the role of KRT17 in liver fibrosis seems necessary.

In the current paper, we explored the role of KRT17 in liver fibrosis both *in vivo* and *in vitro*. We found that KRT17 was upregulated in liver fibrosis. Mechanistically, in hepatic fibrosis, KRT17 promoted the activation of HSCs by inducing EMT, probably via the TGF-β1 pathway. These findings indicate that KRT17 is a valuable indicator and possibly a regulatory biomarker of liver fibrogenesis.

Methods

Animals and induction of hepatic fibrosis

C57BL/6 mice (male, 8 weeks-old) were obtained from the Experimental Animal Center of Nantong Medical University. To establish animal models of hepatic fibrosis, we randomly divided the mice into control and fibrosis groups (10 mice per group). The fibrosis group of mice were administrated with 25% carbon tetrachloride (CCl_4) diluted with olive oil (5 μL/g weight) via intraperitoneal injection biweekly for 8 weeks. The control group of mice received olive oil with equal volume intraperitoneally for the same treatment time. All mice were anesthetized at 24 h after the final injection, then liver samples were extracted to confirm the successful construction of a fibrosis model and for further analysis. All animal experimental protocols were assessed and authorized by the ethics Committee of the Affiliated Hospital of Nantong University.

Human liver specimens

Coupled specimens of fibrotic and corresponding normal human liver tissues were obtained from 16 HCC patients who received surgical operation in the Affiliated Hospital of Nantong University in 2020. Fibrotic liver tissues were excised from para-carcinoma tissues. The protocols for the collection of HCC tissues was authorized by the ethical review committee of the Affiliated Hospital of Nantong University. The age of patients ranged from 25 to 70 years, among them were 9 male and 7 female patients. Every patient had been informed and signed an informed consent form. Liver specimens were immediately frozen in liquid nitrogen after surgical resection.

Hematoxylin and eosin staining

Fresh hepatic tissues were excised from mice, and after fixing in 4% paraformaldehyde for 24 h, they underwent graded ethanol dehydration and paraffin embedding. Sliced hepatic tissues at 5-μm thickness were dewaxed and rehydrated, followed by hematoxylin and eosin (H&E) staining to observe histopathological changes in the fibrotic tissue using light microscopy (H&E, #E607318-0200; BBI Life Sciences, Hong Kong, China).

Sirius red and Masson staining

Liver tissues were also cut with a microtome, and Sirius red and Masson dye staining were employed to determine collagen deposition and fibrosis extent. Liver specimens were acquired under an optical microscope (Olympus Opticals, Tokyo, Japan). Five fields from each liver sample were randomly selected, and the positive red-stained area was semi-quantitatively measured using ImageJ software.

Construction of tissue microarray and immunohistochemical staining

Tissue microarray (TMA) containing 116 para-carcinoma liver tissues was generated from samples collected from HCC patients at the Affiliated Hospital of Nantong University (Nantong, China). Then, cirrhotic and normal liver tissues were obtained for TMA from 60 patients with follow-up data, including 25 cirrhotic and 35 non-fibrotic patients. The 116 adjacent human liver tissues and sliced mice liver sections were fixed in 4% paraformaldehyde and embedded with paraffin (5-μm thick) according to an immunohistochemical staining protocol for histopathological evaluation. Briefly, after deparaffinization in xylene and hydration in an ethanol gradient, liver tissue slices were incubated in sodium citrate buffer for 20 m for antigen retrieval. Then, 3% hydrogen peroxide (H_2O_2) was applied for 20 m to block the endogenous peroxidase activity of the sections. A 10% goat serum was employed to seal up the nonspecific sites by incubating for 1 h at room temperature. After that, the slides were incubated with primary antibody against α-SMA (1:200, ab124964; Abcam, Cambridge, UK), Col1α1 (1:200, ab34710; Abcam), Col3α1 (1:500, ab6310; Abcam) and KRT17 (1:200, ab109725; Abcam) at 4°C for 24 h. After rinsing three times, the slides were incubated with biotinylated secondary antibody at room temperature for 1 h. This was followed by staining with 3, 3′-diaminobenzidine tetrahydrochloride (DAB) to visualize KRT17, α-SMA, Col1α1 and Col3α1 expression. All the sections underwent counterstaining and dehydration. Finally, a microscope was used to observe areas positive for KRT17,

Table 1. Primer sequences used for RT-qPCR

Gene	Forward primer (5′→3′)	Reverse primer (5′→3′)
Mouse		
KRT17	GTTTACCTCCTCCAGCTCTATC	GTAGCAGCTGGAATAACTGTTG
α-SMA	CGGGAGAAAATGACCCAGATT	AGGGACAGCACAGCCTGAATAG
Col1α1	GGAGAGTACTGGATCGACCCTAAC	ACACAGGTCTGACCTGTCTCCAT
GAPDH	TGTTCCTACCCCCAATGTGTCCGTC	CTGGTCCTCAGTGTAGCCCAAGATG
Human		
KRT17	GGTGGGTGGTGAGATCAATGT	CGCGGTTCAGTTCCTCTGTC
α-SMA	AGGCACCCCTGAACCCCAA	CAGCACCGCCTGGATAGCC
Col1α1	CCCGGGTTTCAGAGACAACTTC	TCCACATGCTTTATTCCAGCAATC
Smad2	CCGACACACCGAGATCCTAAC	GAGGTGGCGTTTCTGGAATATAA
E-cadherin	GCTGGACCGAGAGAGTTTCC	CAAAATCCAAGCCCGTGGTG
N-cadherin	GGGAAATGGAAACTTGATGGCA	CAGTTGCTAAACTTCACTGAAAGGA
Vimentin	CGAAACTTCTCAGCATCACG	GCAGAAAGGCACTTGAAAGC
Snail1	TCGGAAGCCTAACTACAAGCGA	AGATGAGCATTGGCAGCGAG
GAPDH	AATGGGCAGCCGTTAGGAAA	GCCCAATACGACCAAATCAGAG

GAPDH, glyceraldehyde-3-phosphate dehydrogenase.

α-SMA, Col1α1 and Col3α1, and immunoreactive cells were quantified using ImageJ software.

Cell culture and treatment

Human immortalized HSCs (the LX-2 cell line) were cultivated in complete Dulbecco's modified Eagle's medium, which contained 10% fetal bovine serum and 1% penicillin-streptomycin (NCM Biotech, Suzhou, China) in an incubator with 5% CO_2 at 37°C. HSC activation was induced by applying recombinant human TGF-β1 (abs04204; Absin, Shanghai, China). When the LX-2 cells' density grew to 80%, they were serum starved for 12 h before 10 ng/mL TGF-β1 treatment. To reverse LX-2 cell activation, they were treated by adipogenic differentiation mixture (MDI; Sigma, St. Louis, MO, USA) for 48 h, which was made up with 0.5 mM isobutylmethylxanthine, 1 μM dexamethasone and 1μM insulin.[32]

Immunofluorescence staining

For immunofluorescence staining, LX-2 cells were inoculated on 24-well plates and cultured in a 37°C incubator. The LX-2 cells were then fixed in 4% paraformaldehyde for 30 m before treatment with 0.5% Triton X-100 for 20 m at room temperature, then blocked with 1% bovine serum albumin for 1.5 h to avoid unspecific staining. Next, the cells were probed with anti-rabbit KRT17 (1:500) and anti-rabbit α-SMA (1:500) diluted in 1% bovine serum albumin at 4°C overnight, followed by peroxidase-conjugated secondary antibodies (1:200) in the dark for 2 h at 37°C. Finally, the nuclei counterstaining was carried out by applying DAPI and the fluorescence was captured using upright fluorescent microscope.

Cell transfection

LX-2 cells were cultured in six-well plates the day before transfection. When the cells were approximately 70% confluent, the medium was converted to serum-free medium in order to transfect with KRT17 overexpressing plasmid and its empty control vectors (TransSheep Bio Co. Ltd, Shanghai, China), small interfering RNA (siRNA) targeting KRT17 (KRT17-siRNA) and its negative control siRNA (siCtrl). Overexpression or knockdown of KRT17 was conducted by applying Lipofectamine 2000 transfection reagent (Invitrogen, Shanghai, China) to LX-2 cells. The KRT17-siRNA and siCtrl were projected and synthesized by Genechem (Shanghai, China). Sequences of the siRNAs used are as follows: KRT17-homo-762 siRNA (sense, 5′-GGUGGGUGGUGAGAUCAAUTT-3′ and antisense, 5′-AUUGAUCUCACCACCCACCTT-3′), KRT17-homo-461 siRNA (sense, 5′-GCCAGUACUACAGGACAAUTT-3′ and antisense, 5′-AUUGUCCUGUAGUACUGGCTT-3′), KRT17-homo-531 siRNA (sense, 5′-CCUGCUACAGAUUGACAAUTT-3′ and antisense, 5′-AUUGUCAAUCUGUAGCAGGTT-3′), negative control siRNA (sense, 5′-UUCUCCGAACGUGUCACGUTT-3′ and antisense, 5′-ACGUGACACGUUCGGAGAATT-3′). The serum-free medium was substituted for complete Dulbecco's modified Eagle's medium at 6 h post-transfection. Cells were harvested after 48 h to confirm the transfection efficiency by real-time quantitative polymerase chain reaction (RT-qPCR) and western blotting. Post-transfected LX-2 cells were harvested for further analysis.

RNA extraction and RT-qPCR

Total RNA from frozen liver tissues or LX-2 cells was extracted by TRIzol reagent (Ambion, Austin, TX, USA), and the concentration of RNA was detected by Nanodrop 8000 (Thermo Fisher Scientific, Waltham, MA, USA). The first-strand cDNA synthesis kit (Vazyme, Nanjing, China) was purchased to reversely transcribe RNA. Subsequently, the RT-qPCR experiment was carried out using a SYBR Green PCR Kit (Qiagen, Hilden, Germany) on a Roche Light Cycler 480 system (Roche Holding AG, Basel, Switzerland) to quantify the mRNA expressions. GAPDH was regarded as an endogenous reference gene. Primer sequences were purchased from Sangon Biotech (Shanghai, China). The primer sequences are listed in Table 1.

Western blot analysis

Cells were lysed in RIPA lysis buffer (Beyotime, Jiangsu, China), then the cell lysate underwent 12,000 rpm centrifugation at 4°C for 10 m to collect the supernatants. The supernatants were boiled at 100°C for 15 m in a 5× sodium dodecyl sulphate loading buffer to obtain protein samples. Proteins were separated on SDS-PAGE and electro-transferred to polyvinyl difluoride membranes (Millipore, Burlington, MA, USA). Followed by application of tris-buffered saline with Tween-20 containing 5% skim milk to block the membranes at room temperature for 1.5 h and incubated with diluted primary antibodies against α-SMA (1:10,000, ab124964; Abcam), Col1α1 (1:1,000, ab34710; Abcam), phospho-Smad2 (1:1,000, 3108P; Cell Signaling Technology, Danvers, MA, USA), Smad2 (1:1,000, 5339P; Cell Signaling Technology), KRT17(1:1,000, ab109725, Abcam), E-Cadherin(1:1,000, 24E10, Cell Signaling Technology), vimentin (1:1,000, D21H3; Cell Signaling Technology), Snail1 (1:1,000, C15D3; Cell Signaling Technology), Smad4 (1:1,000, D3M6Vl Cell Signaling Technology) and GAPDH (1:5,000, 6004-1-Ig; Proteintech, Rosemont, IL, USA) at 4°C for 24 h. After washing with TBST for three times and incubating with species-specific antibodies for 100 m at room temperature, target bands were visualized by a bioimaging system (Bio-Rad, Hercules, CA, USA) using an enhanced chemiluminescent kit (NCM Biotech, Suzhou, China). GAPDH was employed as the internal reference, and finally protein bands were quantified by Image J software.

Cell proliferation assay

LX-2 cells were added to 96-well plates containing 3×10^3 cells per well after transfection with KRT17 overexpressing plasmid and KRT17-siRNA and both their controls for 48 h. Cell vitality was measured by the Cell Counting Kit-8 (CCK-8; Vazyme) at 0, 1, 2 and 3 days. Each well was given a 10 μL aliquot of CCK-8 and cultured in incubator at 37 °C for 4 h before detection. We determined the absorbance at 450 nm on an automated microplate reader (Bio-Rad).

Cell cycle analysis

The Cell Cycle Analysis Kit (Solarbio, Beijing, China) was used to examine cell cycle. Transfected LX-2 cells were collected and washed with pre-cooled phosphate-buffered saline three times, then they were fixed with 70% cold ethanol at 4°C overnight. LX-2 cells were washed by pre-cooled phosphate-buffered saline once again after centrifugation, resuspended with 100 μL RNase A at 37°C to avoid light for 20 m and stained with 200 μL propidium iodide (PI) on ice for 20 m. We employed a flow cytometer (BD Biosciences, Franklin Lakes, NJ, USA) for cell cycle analysis, then cell cycle distributions were quantified by ModFit software package (Verity Software House, Topsham, ME, USA).

Wound healing and Transwell assays

Wound healing and Transwell assays were conducted to affirm cell migration. In wound healing assays, transient transfected LX-2 cells (5×10^5 per well) were added in a six-well plate and cultured in a 37°C incubator. Until they were completely confluent, scratches were created with a 200 μL pipette tip, then the medium was replaced with serum-free medium after washing cells with phosphate-buffered saline three times to remove non-adherent cells. The images of wound areas were photographed at 0 and 24 h under a microscope after scratches were generated. The cell migration rate was quantified by GraphPad Prism 8.0.2 software. For the Transwell assay, 200 μL cell suspensions in serum-free Dulbecco's modified Eagle's medium containing transfected cells (5×10^4 cells) were inoculated to the upper chamber of the Transwell insert (8-μm pore size; Corning, Corning, NY, USA). The lower chamber was inoculated with 600 μL of 20% fetal bovine serum Dulbecco's modified Eagle's medium. At 24 h post-incubation, the unmigrated cells were cleaned with a swab and migrated cells were then fixed in 4% paraformaldehyde and stained with 0.1% crystal violet for 15 m at room temperature. Three randomized views were photographed under an upright microscope and the migratory cells were counted and quantified by the GraphPad Prism 8.0.2 software.

Statistical analysis

The values in our analysis are shown as the mean±standard error (SE). All values were obtained from at least three independent assays. Statistical analyses were conducted with GraphPad Prism 8.0.2 software for Windows. Two-tailed Student's *t*-test was conducted to compare the differences between two groups. A p value less than 0.05 was recognized to be statistically significant.

Results

KRT17 was upregulated in human and mouse liver fibrotic tissues

To explore the role of KRT17 in the development of liver fibrosis, we first measured the expression of KRT17 in human and mouse liver fibrotic tissues. In cirrhotic tissues (n=25) from TMA, the expression of KRT17 was higher than the healthy liver tissues (n=35) from TMA, as measured using immunohistochemistry and qRT-PCR assays (Fig. 1A and 1B). The same result was obtained when KRT17 expression was measured using RT-qPCR and western blotting (Fig. 1C, D). Similarly, the expression of α-SMA, a marker of HSC activation, was significantly higher in liver fibrotic tissues compared to the healthy liver tissues (Fig. 1C, D). Next, we successfully established a mouse model of liver fibrosis by injecting CCl_4 intraperitoneally and verified by means of H&E, Sirius red, and Masson's trichrome staining (Fig. 1E). The immunohistochemical staining revealed that the concomitant expression of KRT17, α-SMA, Col1α1, and Col3α1 along the fibrotic septa were higher in CCl_4-injected livers than the control ones (Fig. 1F). Meanwhile, we also found that the expression of KRT17, α-SMA, and Col1α1 increased in CCl_4-treated mice (Fig. 1G, H). Collectively, our results indicated that KRT17 is associated with HSC activation and collagen deposition, which suggested that KRT17 contributed to the progression of hepatic fibrosis.

KRT17 was elevated in TGF-β1-activated LX-2 cells and restored after MDI treatment in vitro

The expression of KRT17 in liver fibrotic tissues was correlated with α-SMA, and we, therefore, explored the relation between KRT17 expression and HSC activation *in vitro*. LX-2 cells were treated with different concentrations of TGF-β1 recombinant protein for 24 h to induce the activation of HSCs. Following the treatment, it was observed that the expression of α-SMA and Col1α1 was elevated in a dose-depend-

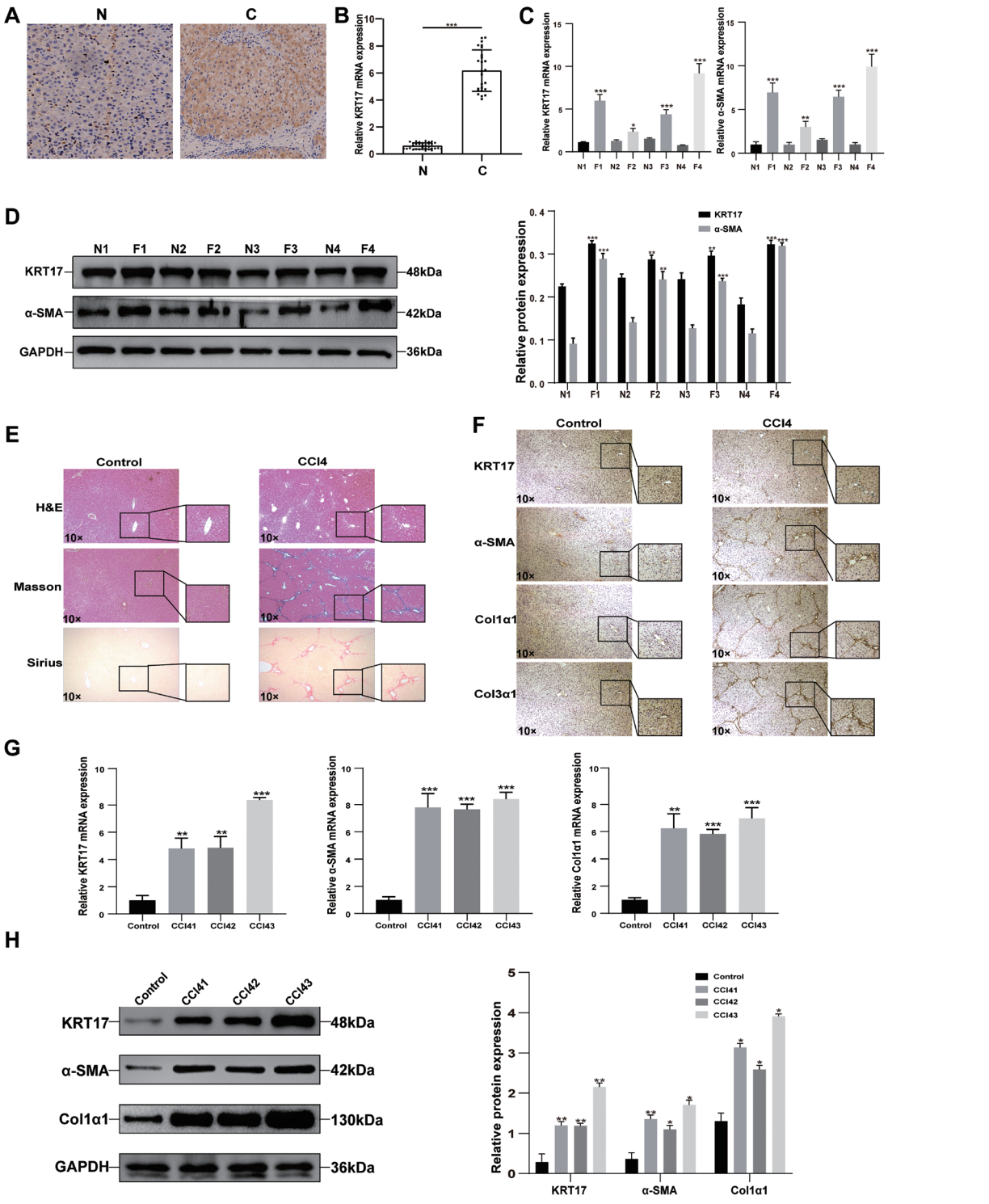

Fig. 1. Upregulation of KRT17 in mouse and human fibrotic livers tissues. (A, B) Randomly selected immunohistochemically stained images of cirrhotic and healthy liver tissues from TMA sections obtained from 60 patients, measuring KRT17 mRNA levels. (C, D) The mRNA and protein levels of KRT17, α-SMA, and Col1α1 in paired fibrotic and corresponding healthy human liver tissues (n=16 patients) measured using RT-qPCR and western blotting analysis. (E) Paraffin-embedded liver sections from olive oil-treated and CCL_4-mediated mouse hepatic tissues (n=10 mice/group) stained with H&E, Masson, and Sirius red. (F) Olive oil-treated and CCL_4-mediated mouse liver tissues (n=10 mice/group) stained using immunohistochemistry against KRT17, α-SMA, Col1α1, and Col3α1. (G, H) The mRNA and protein levels of KRT17, α-SMA, and Col1α1 in olive oil-treated and CCL_4-mediated hepatic tissues (n=10 mice/group) measured using RT-qPCR and western blotting analysis. The results of RT-qPCR are represented as $2^{-\Delta\Delta CT}$ values; N, normal human liver tissues; C, cirrhotic human liver tissues; F, fibrotic human liver tissues; *p<0.05; **p<0.01; ***p<0.001. α-SMA, α-smooth muscle actin; CCl4, carbon tetrachloride; Col1α1, type I collagen alpha 1; Col3α1, type III collagen alpha 1; H&E, hematoxylin and eosin; KRT17, keratin 17; RT-qPCR, real-time quantitative polymerase chain reaction; TMA, tissue microarray.

ent manner (Fig. 2A). Thus, a concentration of 10 ng/mL of TGF-β1 was used in the following experiments. After stimulation with 10 ng/mL of TGF-β1 for the indicated periods, the mRNA and protein levels of α-SMA and Col1α1 in LX-2 cells were detected as early as 6 h and they subsequently increased and peaked at 24 h. Interestingly, KRT17 mRNA and protein levels were unchanged until 24 h of TGF-β1 treatment, which further suggested that KRT17 expression increased in the later stages of HSC activation (Fig. 2B, C). To further affirm the dynamic change in KRT17 expression during the activation of HSCs, we conducted immunofluorescence mono-staining of KRT17 and α-SMA in LX-2 cells treated with TGF-β1 for 0 and 24 h. It was observed that the fluorescence intensities of KRT17 (green) and α-SMA (red) were enhanced at 24 h of TGF-β1 treatment (Fig. 2D). Previous studies have found that myofibroblasts can be reverted to quiescent hepatic stellate cells upon treatment with MDI.[32] We, therefore, incubated LX-2 cells with MDI after TGF-β1 treatment. Compared to treatment with TGF-β1 alone, the protein levels of α-SMA and Col1α1 were lower in LX-2 cells treated with MDI and TGF-β1, demonstrating that the activated LX-2 cells were reverted successfully by MDI *in vitro*. Consistently, KRT17 protein expression was also restored in cells treated with MDI (Fig. 2E). Taken together, these data indicated that KRT17 was positively correlated with the activation of HSCs *in vitro*.

KRT17 promoted the proliferation and migration of LX-2 cells

Considering the increased KRT17 expression in liver fibrotic tissues and its correlation with HSC activation, we wondered whether KRT17 contributed to HSC proliferation and migration. Gain- and loss-of-function analyses were carried out using KRT17-overexpressed plasmid and siRNA targeting KRT17 (KRT17-siRNA), respectively (Fig. 3A). Results of the CCK-8 assay demonstrated that the overexpression of KRT17 promoted the proliferation of LX-2 cells, while knockdown of KRT17 inhibited it (Fig. 3B). To elucidate the underlying mechanism of KRT17-induced increase in LX-2 cell proliferation, we analyzed the cell cycle phase distribution using flow cytometry. The results showed that the overexpression of KRT17 decreased the cells in the G1 phase compared to control, while knockdown of KRT17 induced G1 arrest more prominently compared to the negative control (Fig. 3C, D). Next, cell migration analysis was conducted to explore the impact of KRT17 on the migratory potential of LX-2 cells. Results from the Transwell assay demonstrated that LX-2 cells transfected with KRT17-overexpressed plasmids or siRNA displayed notably increased or reduced migration ability, respectively, compared to the control cells (Fig. 3E, F). In addition, results from the wound healing assay showed that compared with control groups, overexpression or knockdown of KRT17 led to a higher or lower wound closure rate, respectively, in LX-2 cells (Fig. 3G, H). Collectively, these results suggested that KRT17 enhanced the proliferation and migration of LX-2 cells.

KRT17 promoted EMT and the activation of LX-2 cells

It has been previously reported that HSCs can differentiate into collagen-producing myofibroblasts via EMT. We wanted to check whether KRT17 is involved in EMT and HSC activation. We checked the expression of EMT-related genes and α-SMA in LX-2 cells after overexpression or knockdown of KRT17. The results unveiled that the expression levels of E-cadherin, an epithelial cell marker, were downregulated in LX-2 cells transfected with KRT17-overexpressing plasmid, while those of α-SMA and the mesenchymal cell markers N-cadherin, vimentin, and Snail1 were upregulated (Fig. 4A, B). Also, knockdown of KRT17 reduced the expression of α-SMA, N-cadherin, vimentin, and Snail1, and upregulated that of E-cadherin (Fig. 4C, D). These results demonstrated that KRT17 induced EMT and HSC activation.

KRT17 promoted HSC activation via EMT in a TGF-β1-dependent manner

We demonstrated that the expression levels of EMT-related proteins N-cadherin, vimentin, and Snail1 were upregulated in LX-2 cells treated with TGF-β1 recombinant protein in a time-dependent manner (Fig. 5A), and KRT17 regulated EMT (Fig. 4). Since the TGF-β1 signaling pathway plays a pivotal role in EMT progression, we speculated that KRT17-induced HSC activation may correlate with TGF-β1-induced EMT. LX-2 cells were treated with LY2109761, a selective TGF-β1 receptor type I/II (TβRI/II) dual inhibitor, for 24 h after transfection with KRT17-overexpressing plasmid or an empty plasmid as control. The results showed that the upregulated α-SMA, EMT-related proteins, and p-Smad2 induced by KRT17 were counteracted in LX-2 cells treated with LY2109761 (Fig. 5B, C). Our findings implied that TGF-β1 inhibitor partially mitigated the effect of KRT17 on EMT and HSC activation. When we transfected LX-2 cells with siRNA-KRT17 and siRNA-NC before treatment with TGF-β1 for 24 h, we found that knockdown of KRT17 significantly inhibited EMT and the activation of HSCs induced by TGF-β1 (Fig. 5D, E). Given that KRT17 promoted LX-2 cell proliferation and TGF-β1 also triggered HSC proliferation, we suspected KRT17 could induce proliferation of LX-2 cells depending on TGF-β1 signaling. We found that the proliferation of LX-2 cells was prominently impaired in LY2109761-treated cells expressing high levels of KRT17 (Fig. 5F). Collectively, these results indicated that KRT17 facilitated HSC activation via EMT in a TGF-β1-dependent manner, and the proliferation of HSCs induced by KRT17 was also TGF-β1-dependent.

Discussion

Liver fibrosis progresses with the accumulation of ECM proteins and gradually destroys the normal architecture of the hepatic parenchyma, ultimately leading to hepatic dysfunction and more severe consequences.[3,12] For a long time, liver fibrosis was considered intractable because anti-fibrotic drugs exhibited poor patient outcome.[33] Upon liver damage, qHSCs transdifferentiate into collagen-producing myofibroblasts that produce ECM and contribute to liver fibrosis.[34] Hence, suppressing the activation of HSCs has been proposed as a treatment for recovery from liver fibrosis.[35,36] Nevertheless, the underlying molecular mechanisms of this disease and the potential targets for treatment have not been studied in-depth. In the current paper, we focused on the expression and the role of KRT17 in hepatic fibrosis. The results revealed that KRT17 was upregulated in CCl_4-mediated mouse fibrotic liver tissues, human fibrotic liver samples, and TGF-β1-activated LX-2 cells, while it was restored to normal levels after LX-2 cells were inactivated using MDI. The expression of KRT17 was consistent with the markers of activated myofibroblasts (α-SMA and Col1α1). Furthermore, higher expression of KRT17 facilitated proliferation, migration, and activation of HSCs, mediated by EMT via TGF-β1 signaling. The current study reports pioneering results revealing the role of KRT17 in hepatic fibrosis. These findings imply that KRT17 exerts a regulatable function in liver fibrosis and may serve as a potential biomarker for the treatment of hepatic fibrosis.

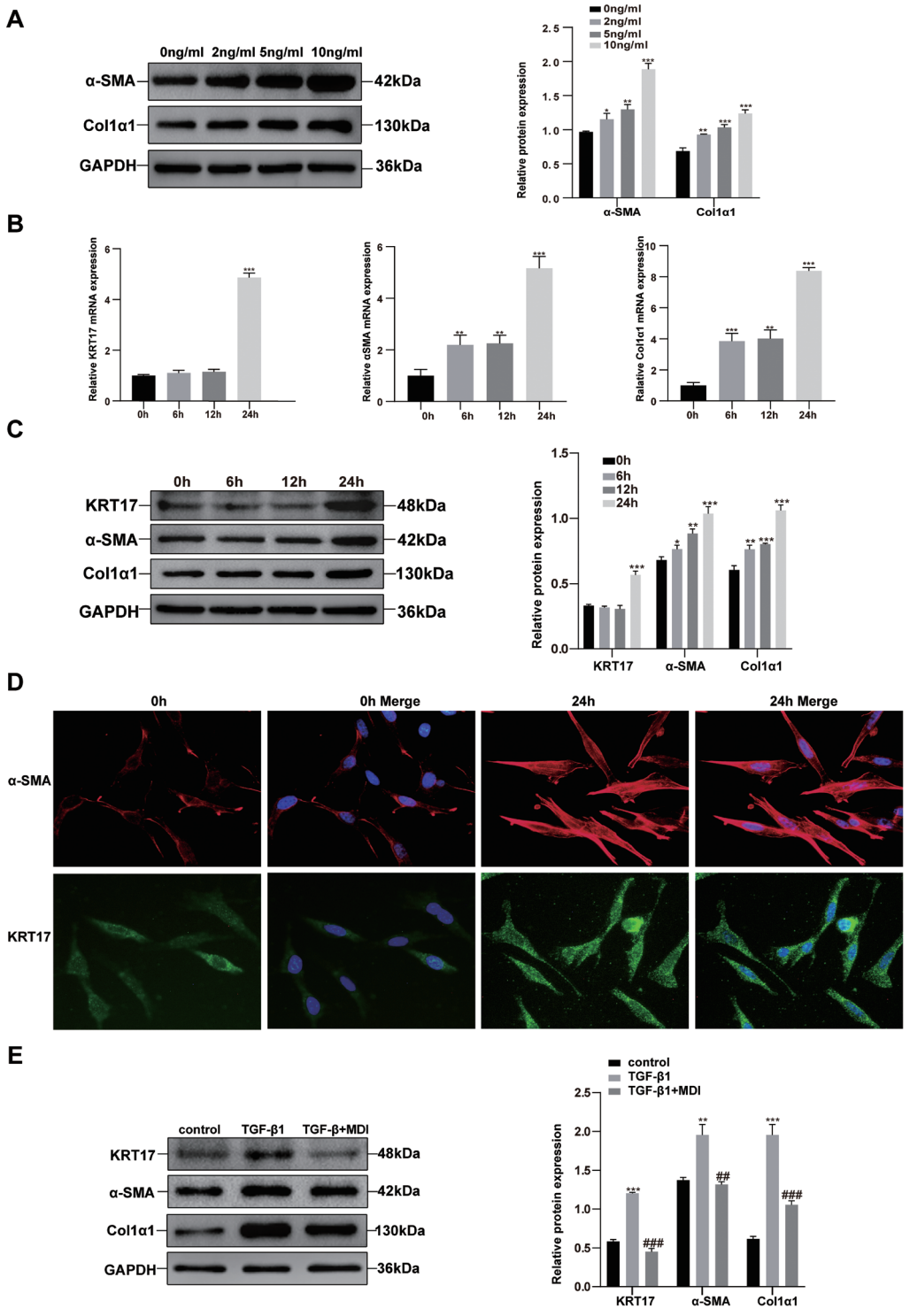

Fig. 2. Increased expression of KRT17 in TGF-β1-activated LX-2 cells and decreased levels of KRT17 after treatment with MDI. (A) LX-2 cells were treated with varying concentrations of TGF-β1 (0, 2, 5, and 10 ng/mL) for 24 h. α-SMA and Col1α1 protein levels were detected using western blotting. (B) Treatment of LX-2 cells with 10 ng/mL TGF-β1 for 0, 6, 12, and 24 h. KRT17, α-SMA, and Col1α1 mRNA levels were measured using RT-qPCR. (C) Treatment of LX-2 cells with 10 ng/mL TGF-β1 for 0, 6, 12, and 24 h. KRT17, α-SMA, and Col1α1 protein levels were measured using western blotting. (D) Immunofluorescence imaging of KRT17 (green) and α-SMA (red) in LX-2 cells at 0 and 24 h after TGF-β1 treatment. (E) Activation of LX-2 cells with the treatment of 10 ng/mL TGF-β1 for 24 h in the model group (activated LX-2 cells) and treatment with MDI for 48 h in the reversal group (reverted LX-2 cells). KRT17, α-SMA, and Col1α1 protein levels in the control group (untreated LX-2 cells), model group, and reversal group were analyzed using western blotting. *p<0.05; **p<0.01; ***p<0.001 vs. control group. $^{\#\#}p$<0.01; $^{\#\#\#}p$<0.001 vs. model group. α-SMA, α-smooth muscle actin; Col1α1, type I collagen alpha 1; KRT17, keratin 17; MDI, adipocyte differentiation mixture; RT-qPCR, real-time quantitative polymerase chain reaction; TMA, tissue microarray.

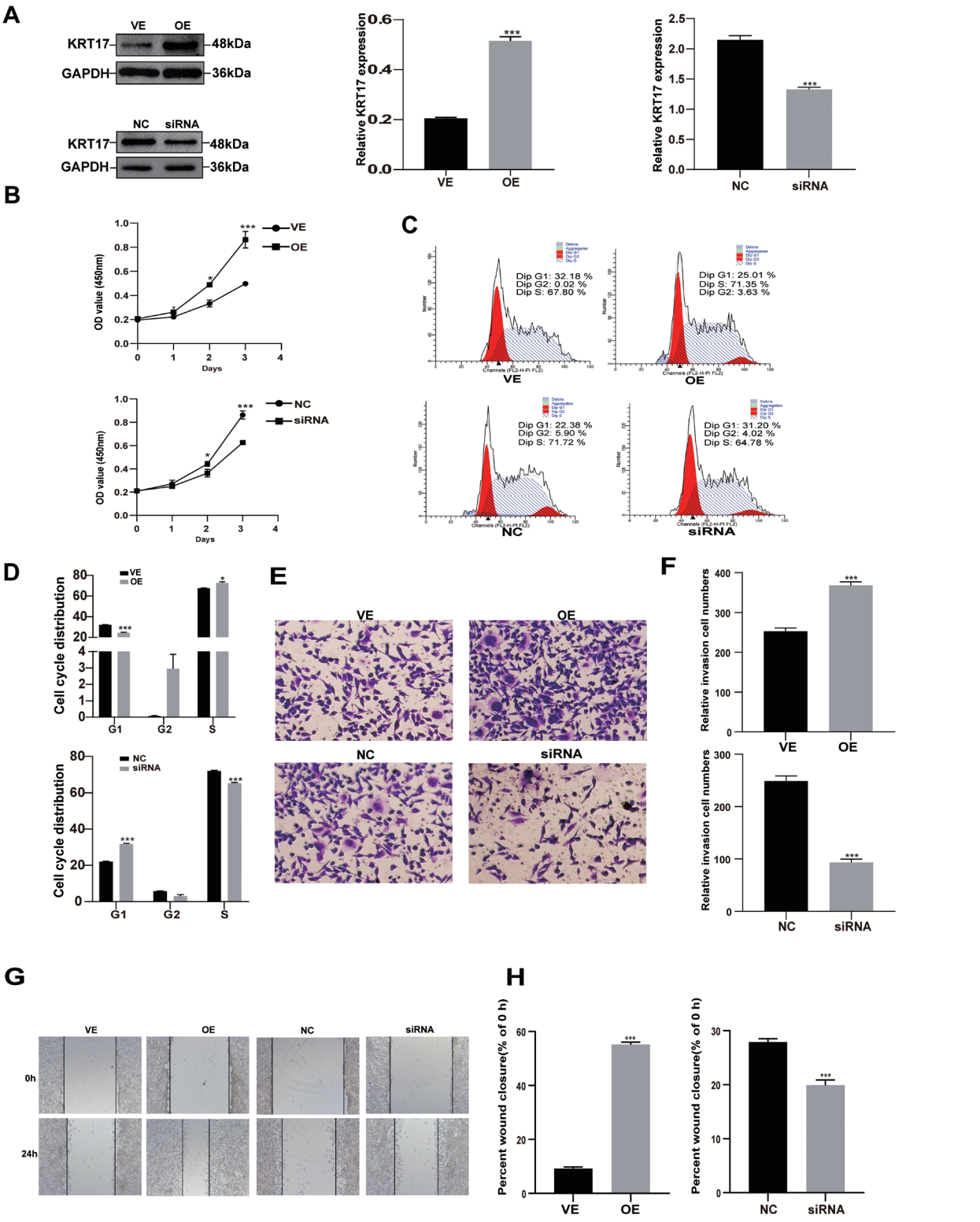

Fig. 3. KRT17 induced proliferation and migration in LX-2 cells. (A) KRT17 expression detected using western blotting after LX-2 cells were transfected with KRT17-overexpressing plasmid, empty-vector controls, siRNA NC, and KRT17-siRNA. (B) Results from the CCK-8 assay showing the LX-2 cell growth curves at 0, 1, 2, and 3 days of culture in the four groups mentioned in (A). (C, D) Results from flow cytometry measuring the distribution of LX-2 cells across the cell cycles in the four groups mentioned in (A). (E, F) Transferability of LX-2 cells as assessed using the Transwell assay after 24 h of culture in the four groups mentioned in (A). (G, H) Migration of LX-2 cells as assessed using the wound-healing assay. Representative microscopy images showing scratch area at the indicated times (0 and 24 h). *p<0.05; ***p<0.001. VE, empty-vector control; OE, KRT17 overexpression; NC, negative control; siRNA, small interfering RNA.

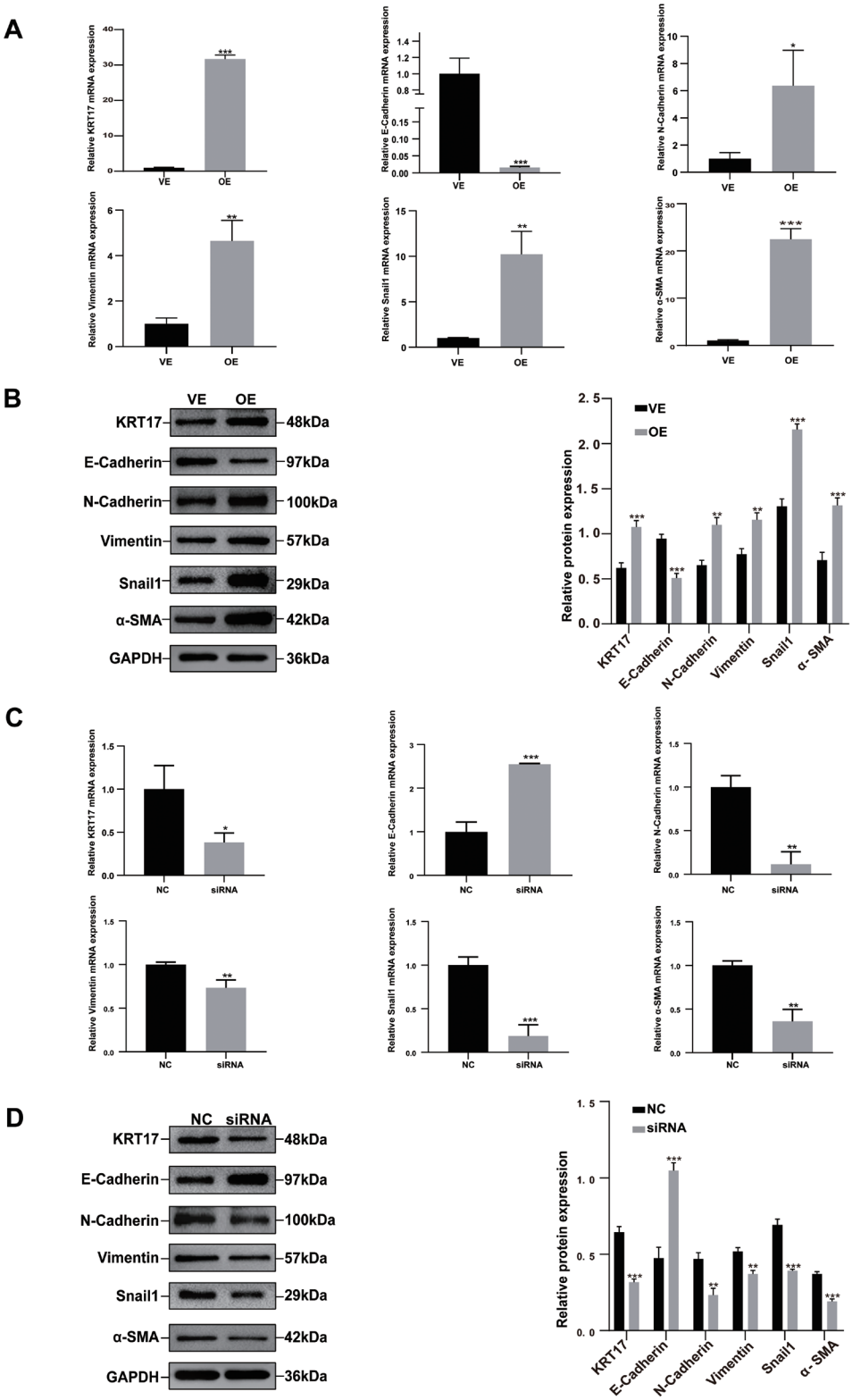

Fig. 4. KRT17 promoted EMT and activated HSCs in LX-2 cells. (A, B) Results from the RT-qPCR and western blotting assays measuring the mRNA and protein levels of EMT-related genes (E-cadherin, N-cadherin, vimentin, and Snail1) and α-SMA in KRT17-overexpressing LX-2 cells and empty vector control cells. (C, D) Results from the RT-qPCR and western blotting assays measuring the relative mRNA and protein levels of EMT-related genes (E-cadherin, N-cadherin, vimentin, and Snail1) and α-SMA in KRT17-knocked down LX-2 cells and negative control cells. *p<0.05; **p<0.01; ***p<0.001. VE, empty-vector control; OE, KRT17 overexpression; NC, negative control; siRNA, small interfering RNA.

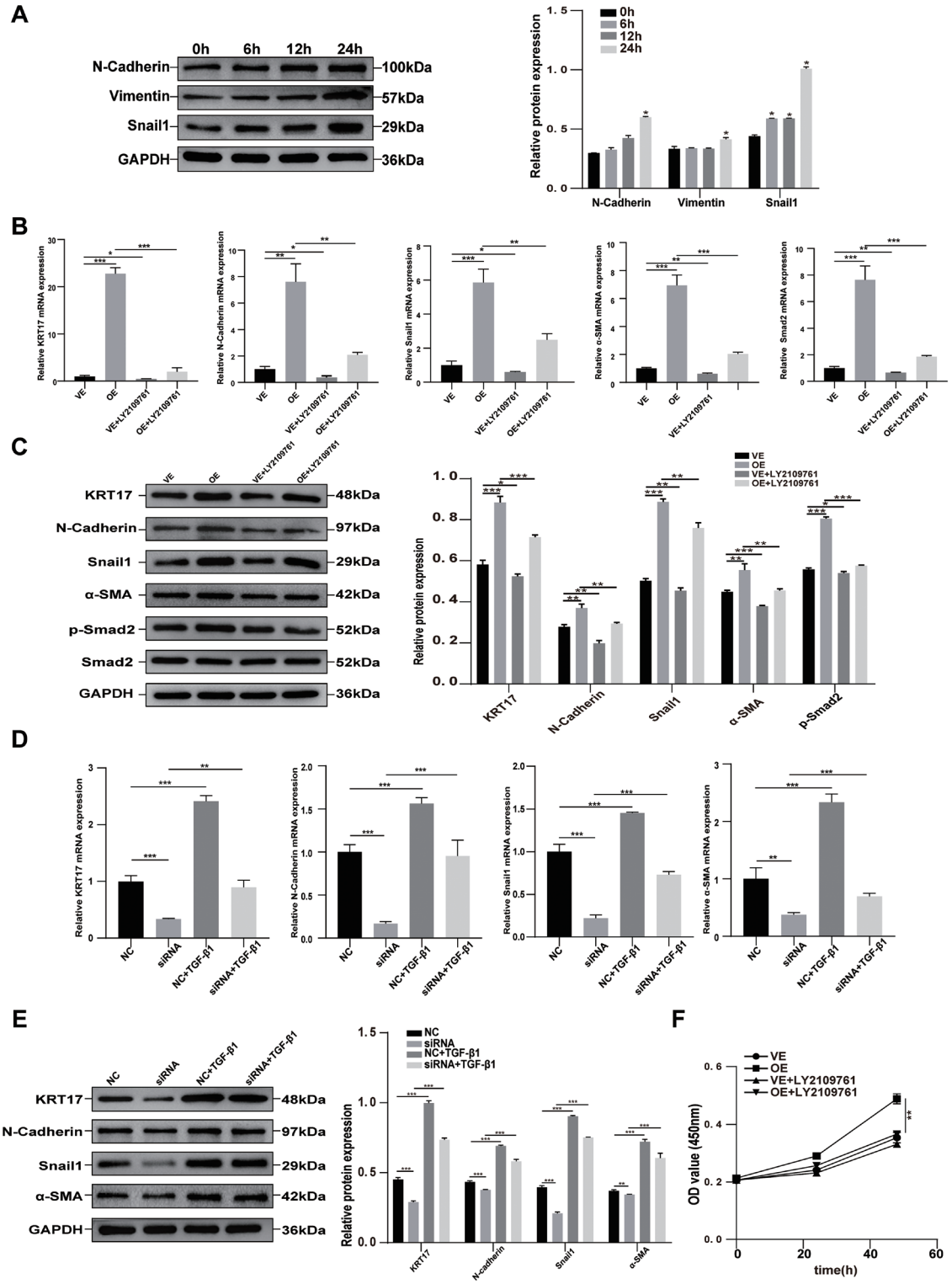

Fig. 5. KRT17 promoted the activation of HSCs via EMT in a TGF-β1-dependent manner. (A) Results of western blotting showing the expression of EMT-related proteins (N-cadherin, vimentin, and Snail1) in LX-2 cells treated with 10 ng/mL of TGF-β1 for 0, 6, 12, and 24 h. (B, C) Results of RT-qPCR and western blotting showing KRT17, N-cadherin, Snail1, α-SMA, and p-Smad2 mRNA and protein levels in LX-2 cells transfected with overexpressed-KRT17 plasmid and the empty vector and then co-treated with 1 uM TGF-β1 inhibitor (LY2109761). (D, E) Results of RT-qPCR and western blotting showing KRT17, N-cadherin, Snail1, and α-SMA mRNA and protein levels in LX-2 cells treated with TGF-β1 for 48 h post-transfection using an overexpressed-KRT17 plasmid, siRNA, and si-NC. (F) Results of the CCK-8 assay showing the proliferation curves of LX-2 cells at 0, 24, and 48 h of culture in these four groups (VE, OE, VE+LY2109761, OE+LY2109761). *p<0.05; **p<0.01; ***p<0.001. VE, empty-vector control; OE, KRT17 overexpression; NC, negative control; siRNA, small interfering RNA.

KRT17, a member of the epithelial keratin family, is involved in multiple biological processes,[37,38] such as cell growth and skin immune response, and is inducible under trauma, epidermal oxidative stress, chemical stimulus, and other pathological conditions.[38] Similarly, upregulation of KRT17 and its pro-oncogenic properties have been shown to positively regulate cancer cell growth, migration, and invasion in several tumors.[30,39] Recent studies have confirmed the involvement of KRT17 in EMT, which can lead to malignancy in tumor cells by inducing invasion and migration.[31] However, the role of KRT17 in hepatic fibrosis is still unknown. In our study, KRT17 expression was upregulated in mouse and human fibrotic livers and correlated with α-SMA expression, which may imply a potential role of KRT17 in HSC activation and EMT. To elucidate the effect of KRT17 on HSCs in-depth, we transiently overexpressed or knocked down KRT17 in LX-2 cells. The results demonstrated that KRT17 overexpression increased LX-2 cell proliferation and migration abilities. Forced expression of KRT17 boosted EMT and HSC activation, along with an increase in the levels of mesenchymal markers (N-cadherin, vimentin, Snail1, and α-SMA) and loss of epithelial biomarkers (E-cadherin) in LX-2 cells. Knockdown of KRT17 inhibited these effects. Thus, we speculated that KRT17 may facilitate hepatic fibrosis by regulating EMT and HSC activation.

TGF-β1 is recognized as a potent pro-fibrogenic cytokine involved in myofibroblast activation.[40] HSCs seldom express TGF-β1 under normal conditions but upon liver injury, its expression increases. Previous research has shown that TGF-β1 also participates in EMT induction, thus facilitating fibrogenesis by promoting the activation of ECM-producing interstitial cells.[22] Consistent with our findings *in vivo*, KRT17 expression was higher in TGF-β1-treated LX-2 cells in a dose- and time-dependent manner, *in vitro*. To confirm the relation between KRT17 and HSC activation, we blocked TGF-β1 signaling using its inhibitor LY2109761 after overexpressing KRT17 in LX-2 cells. We found that forced expression of KRT17 reinforced phosphorylation of Smad2, the effector of the TGF-β1 signaling pathway,[41] accompanied by elevated expression of α-SMA, N-cadherin, vimentin, and Snail1, which was partially relieved by LY2109761. Likewise, inhibition of KRT17 suppressed EMT and the activation of HSCs, and these effects were rescued following treatment by TGF-β1. Taken together, KRT17 activates HSCs via EMT during liver fibrosis, at least in part, through a TGF-β1-dependent mechanism. Several studies have shown that, in addition to the TGF-β1 signaling pathway, the Wnt pathway is also activated in hepatic fibrosis both *in vivo* and *in vitro*, which contributes to the progression of the disease by activating HSCs and EMT.[42–44] Because KRT17 can activate the Wnt pathway and upregulate its core effectors such as β-catenin, C-myc, and CyclinD1 in some diseases,[39] we speculate that the Wnt pathway plays a critical role in promoting the effects of KRT17 on EMT and HSC activation. However, further studies are warranted to elucidate the exact mechanisms.

To sum up, multiple lines of evidence from our current study suggest that KRT17 may mediate EMT and the activation, proliferation, and migration of HSCs by increasing TGF-β1 signaling, consequently accelerating the progression of hepatic fibrosis. To the best of our knowledge, our study is the first to report the regulatory function of KRT17 in hepatic fibrosis. However, our study has a few shortcomings. First, the smaller sample size of 10 C57B/L6 mice per group may have influenced the results. Further studies should be performed using a larger sample size. Second, although the role of KRT17 in liver fibrosis demonstrated in *in vitro* studies cannot be extrapolated to real-life, the use of in-depth technologies, such as KRT17 knockout mice models, are requisites to explore the comprehensive mechanism of KRT17 *in vivo*. Finally, the specific mechanism underlying the regulation of TGF-β1 by KRT17 is poorly understood and other signaling pathways that may be involved remain to be explored.

Looking ahead, KRT17 is involved in the critical processes in the progression of liver fibrosis and is a promising candidate for anti-fibrotic therapies. We aim to further investigate the intricate role of KRT17 in liver fibrosis and the development of anti-fibrotic therapies.

Conclusions

KRT17 was significantly overexpressed in liver fibrosis and restored during its reversal. KRT17 induced EMT and thereby aided in the activation, migration, and proliferation of HSCs, partially via the TGF-β1 signaling pathway. Therefore, KRT17 may be a potential biomarker and target for the treatment of liver fibrosis.

Funding

This study was supported by the National Natural Science Foundation of China, General Project (No. 82070624), Health Commission of Jiangsu Province, Key Project (No. ZDB2020006), Tianqing Liver Disease Research Foundation of China Hepatitis Prevention Foundation (No. TQGB20210029) and Social Development Foundation of Nantong City (No. JC2019032).

Conflict of interest

The authors have no conflict of interests related to this publication.

Author contributions

Study concept and design (CHL, WH), performance of experiments and manuscript drafting (JC, SJG, HJF), specimen collection and data illustration (SZW), and statistical analysis (RJ, WRH). All authors have checked and approved the final manuscript.

Data sharing statement

No additional data are available

References

[1] Bataller R, Brenner DA. Liver fibrosis. J Clin Invest 2005;115(2):209–218. doi:10.1172/JCI24282.
[2] Campana L, Iredale JP. Regression of liver fibrosis. Semin Liver Dis 2017;37(1):1–10. doi:10.1055/s-0036-1597816.
[3] Parola M, Pinzani M. Liver fibrosis: pathophysiology, pathogenetic targets and clinical issues. Mol Aspects Med 2019;65:37–55. doi:10.1016/j.mam.2018.09.002.
[4] Higashi T, Friedman SL, Hoshida Y. Hepatic stellate cells as key target in liver fibrosis. Adv Drug Deliv Rev 2017;121:27–42. doi:10.1016/j.addr.2017.05.007.
[5] Pellicoro A, Ramachandran P, Iredale JP, Fallowfield JA. Liver fibrosis and repair: immune regulation of wound healing in a solid organ. Nat Rev Immunol 2014;14(3):181–194. doi:10.1038/nri3623.
[6] Kisseleva T, Brenner DA. Role of hepatic stellate cells in fibrogenesis and the reversal of fibrosis. J Gastroenterol Hepatol 2007;22(Suppl 1):S73–78. doi:10.1111/j.1440-1746.2006.04658.x.
[7] Wang S, Kim J, Lee C, Oh D, Han J, Kim TJ, *et al*. Tumor necrosis factor-inducible gene 6 reprograms hepatic stellate cells into stem-like cells, which ameliorates liver damage in mouse. Biomaterials 2019;219:119375. doi:10.1016/j.biomaterials.2019.119375.

[8] Pirazzi C, Valenti L, Motta BM, Pingitore P, Hedfalk K, Mancina RM, *et al*. PNPLA3 has retinyl-palmitate lipase activity in human hepatic stellate cells. Hum Mol Genet 2014;23(15):4077–4085. doi:10.1093/hmg/ddu121.
[9] Friedman SL. Mechanisms of hepatic fibrogenesis. Gastroenterology 2008;134(6):1655–1669. doi:10.1053/j.gastro.2008.03.003.
[10] Fuchs BC, Wang H, Yang Y, Wei L, Polasek M, Schuhle DT, *et al*. Molecular MRI of collagen to diagnose and stage liver fibrosis. J Hepatol 2013;59(5):992–998. doi:10.1016/j.jhep.2013.06.026.
[11] Ellis EL, Mann DA. Clinical evidence for the regression of liver fibrosis. J Hepatol 2012;56(5):1171–1180. doi:10.1016/j.jhep.2011.09.024.
[12] Shen H, Sheng L, Chen Z, Jiang L, Su H, Yin L, *et al*. Mouse hepatocyte overexpression of NF-kappaB-inducing kinase (NIK) triggers fatal macrophage-dependent liver injury and fibrosis. Hepatology 2014;60(6):2065–2076. doi:10.1002/hep.27348.
[13] Zhu J, Luo Z, Pan Y, Zheng W, Li W, Zhang Z, *et al*. H19/miR-148a/USP4 axis facilitates liver fibrosis by enhancing TGF-beta signaling in both hepatic stellate cells and hepatocytes. J Cell Physiol 2019;234(6):9698–9710. doi:10.1002/jcp.27656.
[14] Lee YA, Wallace MC, Friedman SL. Pathobiology of liver fibrosis: a translational success story. Gut 2015;64(5):830–841. doi:10.1136/gutjnl-2014-306842.
[15] Griggs LA, Hassan NT, Malik RS, Griffin BP, Martinez BA, Elmore LW, *et al*. Fibronectin fibrils regulate TGF-beta1-induced epithelial-mesenchymal transition. Matrix Biol 2017;60-61:157–175. doi:10.1016/j.matbio.2017.01.001.
[16] Thiery JP. Epithelial-mesenchymal transitions in tumour progression. Nat Rev Cancer 2002;2(6):442–454. doi:10.1038/nrc822.
[17] Kalluri R, Neilson EG. Epithelial-mesenchymal transition and its implications for fibrosis. J Clin Invest 2003;112(12):1776–1784. doi:10.1172/JCI20530.
[18] Pinzani M. Epithelial-mesenchymal transition in chronic liver disease: fibrogenesis or escape from death? J Hepatol 2011;55(2):459–465. doi:10.1016/j.jhep.2011.02.001.
[19] Zavadil J, Bottinger EP. TGF-beta and epithelial-to-mesenchymal transitions. Oncogene 2005;24(37):5764–5774. doi:10.1038/sj.onc.1208927.
[20] Choi SS, Diehl AM. Epithelial-to-mesenchymal transitions in the liver. Hepatology 2009;50(6):2007–2013. doi:10.1002/hep.23196.
[21] Ding ZY, Jin GN, Liang HF, Wang W, Chen WX, Datta PK, *et al*. Transforming growth factor beta induces expression of connective tissue growth factor in hepatic progenitor cells through Smad independent signaling. Cell Signal 2013;25(10):1981–1992. doi:10.1016/j.cellsig.2013.05.027.
[22] Nitta T, Kim JS, Mohuczy D, Behrns KE. Murine cirrhosis induces hepatocyte epithelial mesenchymal transition and alterations in survival signaling pathways. Hepatology 2008;48(3):909–919. doi:10.1002/hep.22397.
[23] Karantza V. Keratins in health and cancer: more than mere epithelial cell markers. Oncogene 2011;30(2):127–138. doi:10.1038/onc.2010.456.
[24] Jacob JT, Coulombe PA, Kwan R, Omary MB. Types I and II keratin intermediate filaments. Cold Spring Harb Perspect Biol 2018;10(4):a018275. doi:10.1101/cshperspect.a018275.
[25] Chivu-Economescu M, Dragu DL, Necula LG, Matei L, Enciu AM, Bleotu C, *et al*. Knockdown of KRT17 by siRNA induces antitumoral effects on gastric cancer cells. Gastric Cancer 2017;20(6):948–959. doi:10.1007/s10120-017-0712-y.
[26] Kurokawa I, Takahashi K, Moll I, Moll R. Expression of keratins in cutaneous epithelial tumors and related disorders-distribution and clinical significance. Experimental dermatology 2011;20(3):217–228. doi:10.1111/j.1600-0625.2009.01006.x.
[27] McGowan KM, Coulombe PA. Onset of keratin 17 expression coincides with the definition of major epithelial lineages during skin development. J Cell Biol 1998;143(2):469–486. doi:10.1083/jcb.143.2.469.
[28] van de Rijn M, Perou CM, Tibshirani R, Haas P, Kallioniemi O, Kononen J, *et al*. Expression of cytokeratins 17 and 5 identifies a group of breast carcinomas with poor clinical outcome. Am J Pathol 2002;161(6):1991–1996. doi:10.1016/S0002-9440(10)64476-8.
[29] Moll R, Divo M, Langbein L. The human keratins: biology and pathology. Histochem Cell Biol 2008;129(6):705–733. doi:10.1007/s00418-008-0435-6.
[30] Chiang CH, Wu CC, Lee LY, Li YC, Liu HP, Hsu CW, *et al*. Proteomics analysis reveals involvement of Krt17 in areca nut-induced oral carcinogenesis. J Proteome Res 2016;15(9):2981–2997. doi:10.1021/acs.jproteome.6b00138.
[31] Sankar S, Tanner J, Bell R, Chaturvedi A, Randall R, Beckerle M, *et al*. A novel role for keratin 17 in coordinating oncogenic transformation and cellular adhesion in Ewing sarcoma. Mol Cell Biol 2013;33(22):4448–4460. doi:10.1128/mcb.00241-13.
[32] She H, Xiong S, Hazra S, Tsukamoto H. Adipogenic transcriptional regulation of hepatic stellate cells. J Biol Chem 2005;280(6):4959–4967. doi:10.1074/jbc.M410078200.
[33] Bataller R, Brenner D. Liver fibrosis. J Clin Invest 2005;115(2):209–218. doi:10.1172/jci24282.
[34] Hernandez-Gea V, Friedman S. Pathogenesis of liver fibrosis. Annu Rev Pathol 2011;6:425–456. doi:10.1146/annurev-pathol-011110-130246.
[35] Mederacke I, Hsu C, Troeger J, Huebener P, Mu X, Dapito D, *et al*. Fate tracing reveals hepatic stellate cells as dominant contributors to liver fibrosis independent of its aetiology. Nat Commun 2013;4:2823. doi:10.1038/ncomms3823.
[36] Wu J, Liu L, Yen R, Catana A, Nantz M, Zern M. Liposome-mediated extracellular superoxide dismutase gene delivery protects against acute liver injury in mice. Hepatology 2004;40(1):195–204. doi:10.1002/hep.20288.
[37] Yang L, Zhang S, Wang G. Keratin 17 in disease pathogenesis: from cancer to dermatoses. J Pathol 2019;247(2):158–165. doi:10.1002/path.5178.
[38] Kim S, Wong P, Coulombe P. A keratin cytoskeletal protein regulates protein synthesis and epithelial cell growth. Nature 2006;441(7091):362–365. doi:10.1038/nature04659.
[39] Wang Z, Yang M, Lei L, Fei L, Zheng Y, Huang W, *et al*. Overexpression of KRT17 promotes proliferation and invasion of non-small cell lung cancer and indicates poor prognosis. Cancer Manag Res 2019;11:7485–7497. doi:10.2147/cmar.s218926.
[40] Kisseleva T, Brenner D. Hepatic stellate cells and the reversal of fibrosis. J Gastroenterol Hepatol 2006;21(Suppl 3):S84–87. doi:10.1111/j.1440-1746.2006.04584.x.
[41] Carthy J. TGFβ signaling and the control of myofibroblast differentiation: implications for chronic inflammatory disorders. J Cell Physiol 2018;233(1):98–106. doi:10.1002/jcp.25879.
[42] Ge W, Wang Y, Wu J, Fan J, Chen Y, Zhu L. β-catenin is overexpressed in hepatic fibrosis and blockage of Wnt/β-catenin signaling inhibits hepatic stellate cell activation. Mol Med Rep 2014;9(6):2145–2151. doi:10.3892/mmr.2014.2099.
[43] Monga S. β-catenin signaling and roles in liver homeostasis, injury, and tumorigenesis. Gastroenterology 2015;148(7):1294–1310. doi:10.1053/j.gastro.2015.02.056.
[44] Zhang M, Miao F, Huang R, Liu W, Zhao Y, Jiao T, *et al*. RHBDD1 promotes colorectal cancer metastasis through the Wnt signaling pathway and its downstream target ZEB1. J Exp Clin Cancer Res 2018;37(1):22. doi:10.1186/s13046-018-0687-5.